*International Journal of Geosciences*, **2011, 2, 676-688**
doi:10.4236/ijg.2011.24069 Published Online November 2011 (http://www.SciRP.org/journal/ijg)

# Imaging the Deep Structure of the Central Death Valley Basin Using Receiver Function, Gravity, and Magnetic Data

**Musa Hussein, Laura Serpa, Aaron Velasco, Diane Doser**
[1]*Department of Geological Sciences, University of Texas at El Paso, El Paso, USA*
*E-mail*: *mjhussein@utep.edu*
*Received September* 17, 2011; *revised October* 9, 2011; *November* 5, 2011

## Abstract

We use receiver function, gravity, and magnetic data to image the deep structures of central Death Valley. Receiver function analysis suggests the Moho is 24 km deep in the central part of the basin and deepens to 33 km to the east and 31 km to the west. The estimated lower crustal density is 2900 kg/m$^3$, which suggests a gabbroic composition, whereas the upper crustal density, excluding basin sediments, is estimated to average 2690 kg/m$^3$ or approximately a quartzofeldspathic composition. We modeled the magnetic sources as upper crustal to suggest a relatively shallow Curie depth in this region of high heat flow. We developed models to test the hypothesis that a low-density, non-magnetic body (magma or fluid-rich material?) within the lower crust at a depth of 15 km could coincide with the location of the Death Valley bright spot imaged on a deep seismic reflection profile. Those models suggest that if there is a low density region in the mid to lower crust in the area of the bright spot, then the region is also likely to be underplated by mafic or ultramafic materials which may have contributed to heating, uplift, and thinning of the crust during extension.

**Keywords:** Bright Spot, Crustal Models, Data Incorporation, Death Valley, Magmatic Underplating

## 1. Introduction

Death Valley (**Figure 1**) is a deep topographic basin that extends for approximately 200 km in a north-northwest direction in southeastern California. It represents an ideal region to study basin evolution and structure because it is actively deforming, there is little vegetation, and the sedimentation rates are low. As a result of these attributes, numerous models have been developed to describe the basin evolution and to determine which processes may be important in that evolution [1-7]

Of particular interest here is the presence of a high amplitude seismic reflection anomaly, termed the Death Valley "bright spot" [8] (**Figure 1**) which has been suggested to be associated with a magmatic intrusion and volcanism in central Death Valley. Reference [9] did not find evidence for such a feature elsewhere in the region in his seismic studies and, similarly, a magnetotelluric study [10,11] north of the seismic study area did not find supporting evidence for magma in the crust. These studies suggest that if the bright spot is due to a magma body beneath central Death Valley, it is not regionally extensive and is probably relatively small or includes very little actual molten material.

To study the bright spot, we used receiver function, gravity, and magnetic data combined with preexisting seismic reflection models of [2,12] to produce crustal models of the Death Valley region around the inferred bright spot. The bright spot can be associated with a magma body in the Death Valley subsurface and magma may extend from the surface into the upper mantle where it may be associated magmatic underplating of a large region around the Central Death Valley basin.

## 2. Tectonic Setting

Death Valley is a pull-apart basin [13] formed at a right stepping bend in the right-lateral Death Valley fault system. The transtensional process has exhumed a complex crystalline terrane in the Black Mountains along the eastern side of Death Valley. Crystalline assemblages are separated from the floor of Death Valley by a system of late Cenozoic faults that include young scarps in alluvial fans [14,15].

 

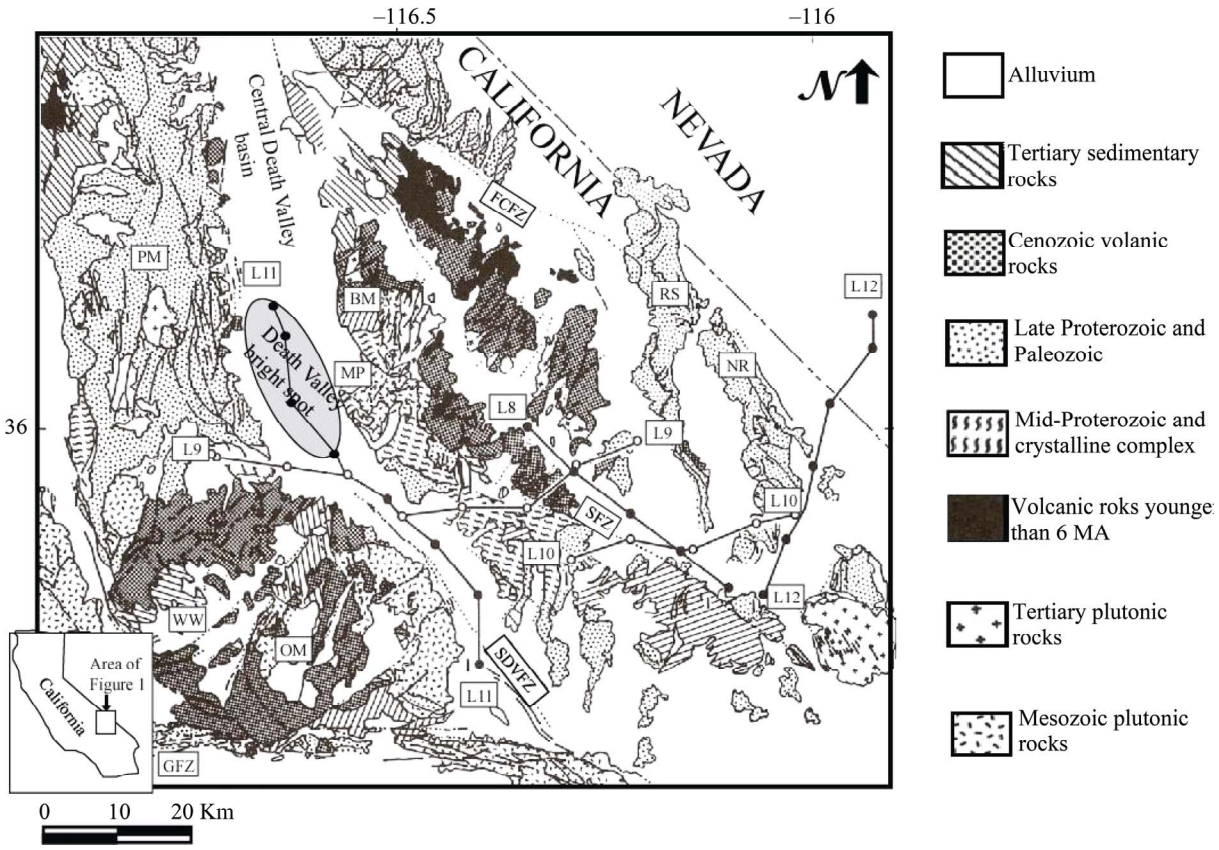


**Figure 1.Generalized geologic map of the Death Valley (after Wright and Troxel, 1973). The following abbreviations are used throughout the figures: FCFZ, Furnace Creek fault zone; BM, Black Mountains; MP, Mormon Point; OM, Owlshead Mountains; PM, Panamint Mountains; NR, Nopah Range; RS, Resting Spring; SDVFZ, Southern Death Valley Fault zone; SFZ, Sheephead fault zone; WW, Wingate Wash fault zone. The location of Consortium for Continental Reflection Profiling (COCORP) lines L8 through L12 are indicated by the bold lines. The gray oval indicates the location of the Death Valley bright spot.**

The central Death Valley basin is a half-graben faulted along the Black Mountains to the east of the basin [2,15,16]. This structural geometry is supported by the eastward tilt of the Badwater saltpan, and by the asymmetry of alluvial-fan size and shape from one side of the valley to the other [17] and by geophysical data [2,17-19]. The geophysical data indicate that the valley fill consists of approximately 3 km of alluvium, lacus- trine, volcanic, and evaporite deposits.

The Consortium for Continental Reflection Profiling (COCORP) collected 250 km of deep seismic reflection data in the vicinity of Death Valley, California [8,20] **Figure 1** shows the location of COCORP lines 9 and 11 within central Death Valley. These profiles provided information on the upper crustal fault blocks, as well as other features of the deep crust and upper mantle associated with the development of the central Death Valley pull-apart basin and surrounding area. References [8,21] interpreted a strong reflecting zone at mid-crustal depth, termed the Death Valley bright spot, as evidence of magma in the middle crust. Reference [2] traced the bright spot reflections to the surface location of a young volcanic cone and interpreted a mid-crustal reflective zone at approximately 15 km depth in central Death Valley, including the bright spot, to suggest the reflecting horizon is domed upward beneath the basin [22].

Unusually strong reflections can be generated in several ways: 1) focusing of seismic energy by structural curvature or velocity lenses, 2) constructive interference (tuning), or 3) a juxtaposition of materials with a large acoustic impedance contrast [8,23]. The unusually high reflection amplitude for the Death Valley bright spot could represent the accumulation of magma in the middle crust [8] or other fluids [24]. Additionally, [25] interpreted the magma source for the cinder cone that [2] connected to the bright spot to have originated near the base of the crust following the model of [26]. Reference [26] suggested that magmas can underplate extensional regions and that the mafic igneous rocks that are found in those regions are the product of differentiation from the

 

underplated magma source.

## 3. Data

### 3.1. Receiver Functions

A receiver function is the seismic response of the earth beneath a seismic station to an incoming *P*-wave. In particular, a receiver function maps *P*-to-*S* converted energy that occurs from impedance contrasts (*i.e*., layers of different velocity and density) in the earth. First-order information about the crustal structure can be derived from the radial receiver function, which is dominated by *P*-to-*S* converted energy from a series of velocity discontinuities in the crust and upper mantle [27]. Thus, receiver functions can provide very good point measurements of crustal thickness under a broadband station. Because of the large velocity contrast at the crust-mantle boundary, the Moho *P*-to-*S* conversion (*Ps*) is often the largest signal following the direct P-wave [28]. Receiver functions can be used to determine crustal thickness and $V_p/V_s$ ratios, and to determine the lateral variation of the Moho depth [28]. For example, in regions of lithospheric extension, one would expect to find a thin crust and therefore a shallow Moho.

We employ the receiver function technique using the iterative deconvolution method of [29] and the stacking approach described in [28]. In receiver function estimation, the foundation of the iterative deconvolution approach is least squares minimization of the difference between the observed horizontal component seismogram and predicted signal generated by convolution of an iterative updated spike train with the vertical component seismogram [29].

The iterative time-domain approach has several advantages, such as the ability to estimate the percent fit and the long period stability by *a priori* constructing the deconvolution as a sum of Gaussian pulses [29]. We compute receiver functions using the iterative time deconvolution with Gaussian width (Ga) factors of 2.5, 1.75, and 1 which is equivalent to applying low pass filters with cutoff frequencies of 1.2, 0.9, and 0.5 Hz, respectively.

We collected waveforms of teleseismic earthquakes with M > 5.5 from 13 broadband seismograph stations (listed in **Table 1** and shown in **Figure 2**) that recorded from 2000 to 2009. These data were downloaded directly from the Incorporated Research Institutes for Seismology (IRIS) Data Management Center using the Standing Order of Data, which allowed for automated rotation of the horizontal components to radial and transverse directions. From the waveform data, we computed the radial and transverse receiver functions using the iterative deconvolution method, keeping data with an 80% or greater fit. We also manually inspected each radial receiver function to ensure quality. We then stacked the radial receiver functions using the approach of [28].

The time separation *t* between *Ps* and *P* can be used to estimate crustal thickness (*H*), given the average crustal velocity:

$$H = \frac{t_{Ps}}{\sqrt{1/V_s^2 - p^2} - \sqrt{1/V_p^2 - p^2}}$$

**Table 1. Receiver function station codes, $V_p/V_s$ ratios, depth to the Moho, and number of receiver functions.**

| Station | Longitudes | Latitudes | Est. $V_p/V_s$ | Est. Thickness | No of RF |
|---|---|---|---|---|---|
| Cl-FUR | −116.86 | 36.47 | 2.02 ± 0.09 | 23.47 ± 0.42 | 336 |
| Cl-MPM | −117.49 | 36.06 | 1.78 ± 0.09 | 26.43 ± 0.33 | 554 |
| Cl-GSC | −116.81 | 35.3 | 1.95 ± 0.11 | 25.43 ± 0.44 | 439 |
| Cl-GRA | −117.37 | 37 | 1.7 ± 0.09 | 33.50 ± 0.45 | 252 |
| Cl-LRL | −117.68 | 35.48 | 1.76 ± 0.10 | 30.53 ± 0.36 | 197 |
| Cl-EDW2 | −118.0 | 34.9 | 1.75 ± 0.10 | 30.03 ± 0.30 | 188 |
| Cl-CWC | −118.1 | 36.4 | 1.9 ± 0.13 | 31.06 ± 0.50 | 195 |
| Cl-HEC | −116.3 | 34.8 | 1.79 ± 0.09 | 28.44 ± 0.27 | 141 |
| Cl-RRX | −117.0 | 34.9 | 1.88 ± 0.10 | 31.49 ± 0.33 | 194 |
| Cl-TIN | −118.2 | 37.1 | 1.70 ± 0.08 | 35.47 ± 0.27 | 227 |
| Cl-SHO | −116.28 | 35.9 | 1.85 ± 0.13 | 29.41 ± 0.25 | 126 |
| US-TPNV | −116.25 | 36.95 | 1.62 ± 0.08 | 33.97 ± 0.20 | 123 |
| TA-U10A | −116.3 | 36.4 | 1.89 ± 0.08 | 31.39 ± 0.60 | 34 |

 

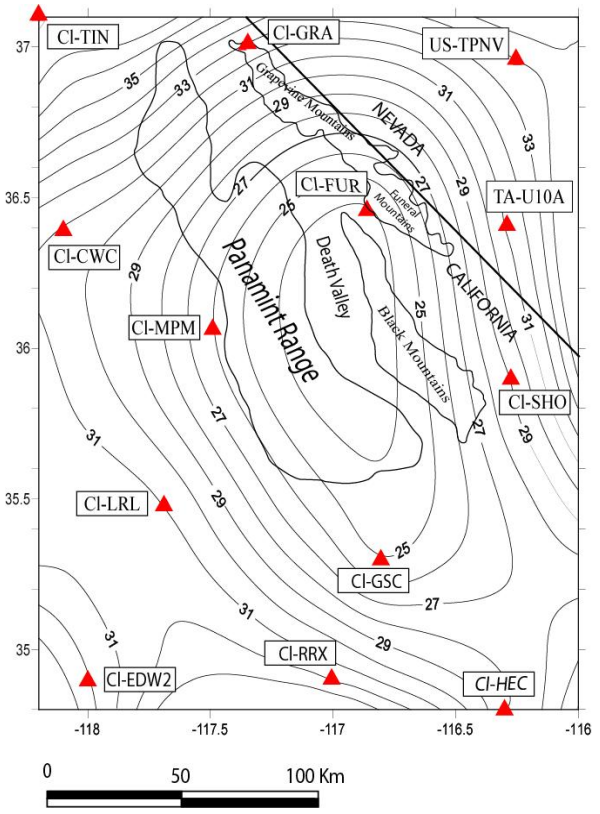


**Figure 2. Contour map of the Moho depth (km) in Death Valley based on receiver function data. Data were collected from 13 stations (shown as triangles). Stations codes are shown inside small squares beside each station.**

where $p$ is the ray parameter of the incident wave. One problem is the trade-off between the thickness and crustal velocities, since $t_{Ps}$ represents the differential travel time of $S$ with respect to $P$ wave in the crust. The dependence of ($H$) on $V_p$ is not as strong as on $V_s$ or more precisely on the $V_p/V_s$ ratio ($K$), which means the uncertainty of ($H$) is <0.5 km for a 0.1 km/s uncertainty in $V_p$; while a 0.1 change in ($K$) can lead to about 4 km change in the crustal thickness [28].

This ambiguity can be reduced by using a later phase, which provides additional constraints so that both ($K$) and ($H$) can be estimated [30-32].

**Figure 3** shows *H-K* stacks for selected stations within the study area; the results for the stacks give good estimates of the crustal thickness and the $V_p/V_s$ ratio. We find that our stacking results differ slightly (difference ranges from 0 to 4 km) for several stations compared to those reported from the Earth Scope Automated Receiver Survey (EARS). The reasons for this are likely the following: different selection criteria, differing amounts of data, and different quality control. Using the results from receiver functions, we contour the Moho depth (**Figure 2**) using a minimum-curvature algorithm to interpolate values

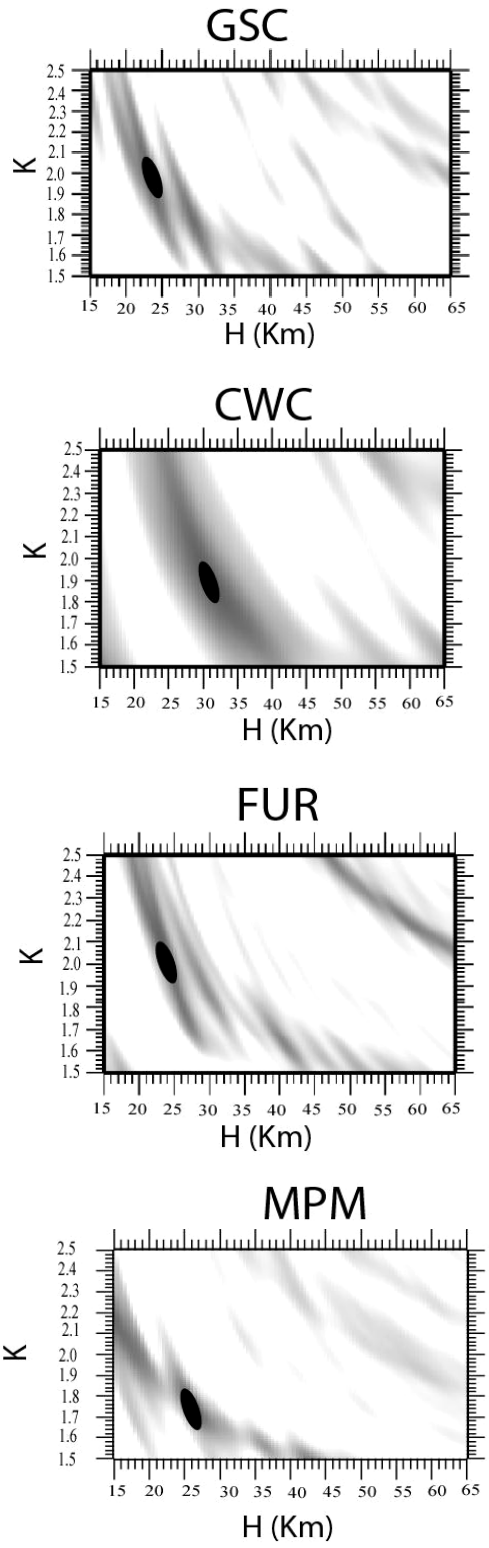


**Figure 3. H-K stacks for stations GSC, CWC, FUR, and MPM. The black ovals represent the maximum value of the H-K stacks. Depth to Moho is 25, 31, 24 and 26 km according to stations GSC, CWC, FUR, and MPM, respectively. See Figure 2 for station locations.**

 

to a rectangular grid. Although no stations fall within Death Valley, there is clear evidence that Moho depth decreases toward the valley based on the trends from the stations located closest to the valley. In particular, there is a station (CI-FUR in **Figure 2** and **Table 1**) near the northern end of central Death Valley that clearly shows the shallowest Moho at less than 24 km depth in the area. Thus, the Moho appears to have a dome shape, with Moho depth decreasing from approximately 31 km outside the Valley to 20 - 25 km in central Death Valley, assuming a relatively uniform rate of change from the areas where the stations are located.

The $V_p/V_s$ ratio (**Table 1**) ranges from 2 to 1.91 in central Death Valley and from 1.85 to 1.73 in the other areas. The major factor producing high $V_p/V_s$ is the plagioclase-rich mafic composition of the lower crust [33]. Reference [34] concluded that a low $V_p$ velocity combined with low $V_p/V_s$ zones in the upper crust are caused by the inclusion of $H_2O$ and that a low $V_p$ velocity with high $V_p/V_s$ zones in the lower crust and the uppermost mantle are caused by melt inclusions. That model suggests the high $V_p/V_s$ ratio in the lower crust is indicative of a mafic lower crustal composition but we do not have an independent measure of $V_p$ to use to determine whether there is magma in the crust.

### 3.2. Gravity and Aeromagnetic Data

We obtained gravity data from the University of Texas at El Paso (UTEP) -Pan American Center of Earth and Environmental Studies-(PACES) that is currently hosted at the CYBER-ShARE Center of Excellence at UTEP (http://www.research.utep.edu/paces). The gravity data were merged from a variety of surveys and cover the U.S. and the border region. The average error for this data set ranges from 0.05 to 2mGal (Al-Douri, personal communication, 2009). Terrain corrections were calculated by [35] of the U. S. Geological Survey (USGS) using a digital elevation model and a technique based on the approach of [36].

A Bouguer gravity correction was made using 2670 kg/m$^3$ as the reduction density. We used 7,930 Bouguer gravity points to create the Bouguer gravity anomaly map (**Figures 4** and **5)**. Aeromagnetic data were obtained from the U.S. Geological Survey with a grid spacing of 1 km [37]. We used a total of 36,342 digitized aeromagnetic points to create the magnetic anomaly map (**Figure 6)**.

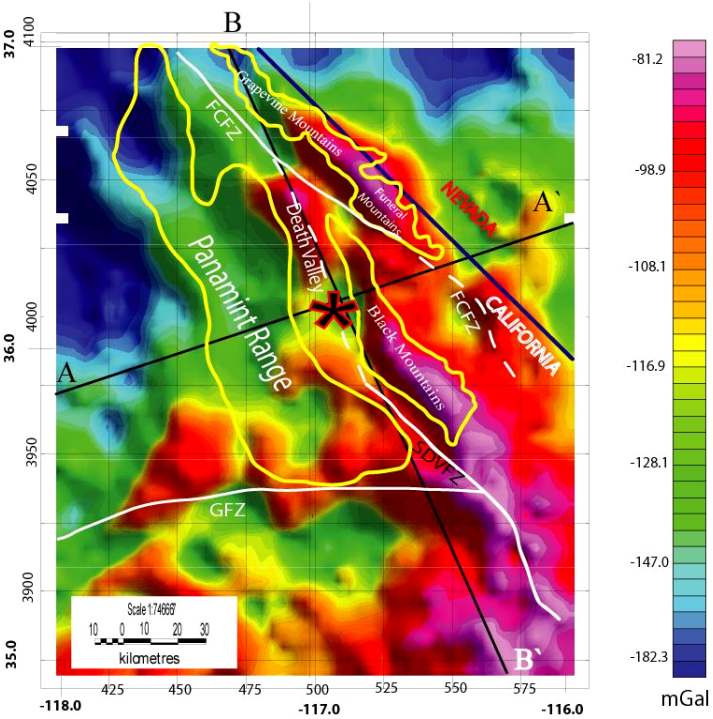


**Figure 4. Bouguer anomaly map of the Death Valley area. The *marks a gravity low (–120 to –130 mGal), which coincides with the Death Valley bright spot location. Large amplitude gravity anomalies are observed along the southern Death Valley fault zone (SDVFZ) and to the southeast. Note the well defined alignment of anomalies along the Garlock fault zone. Solid lines A-A` and B-B` show the location of the gravity profiles shown in Figures 8 and 9. The locations of the profiles were chosen to illustrate the general crustal structure of the study area. FCFZ, Furnace Creek fault zone; SDVFZ, Southern Death Valley Fault zone; GFZ, Garlock Fault Zone.**

 

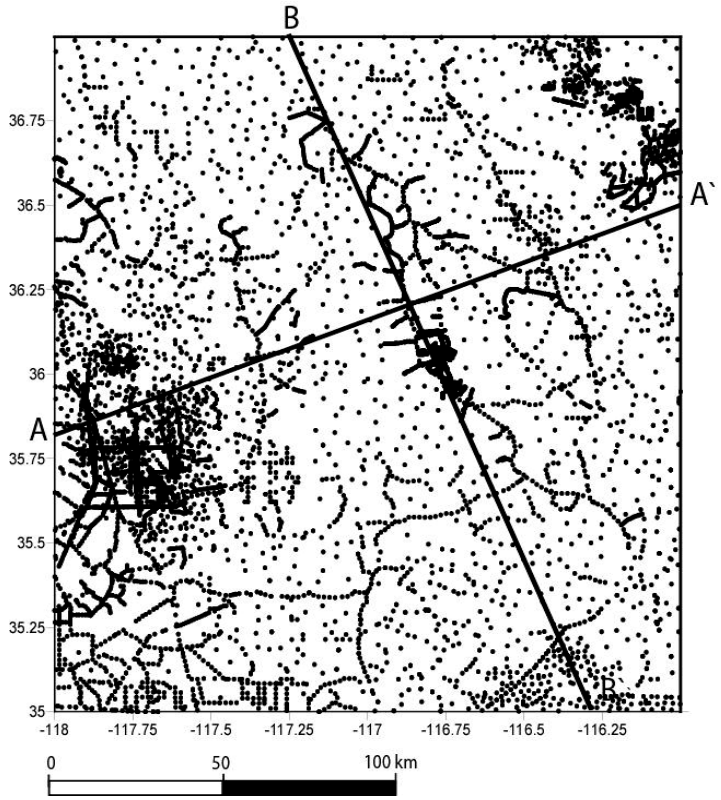


**Figure 5. Gravity stations location map, solids lines show location of gravity profiles shown in Figures 8 and 9. The study area covered wit total of (7930) gravity measurements.**

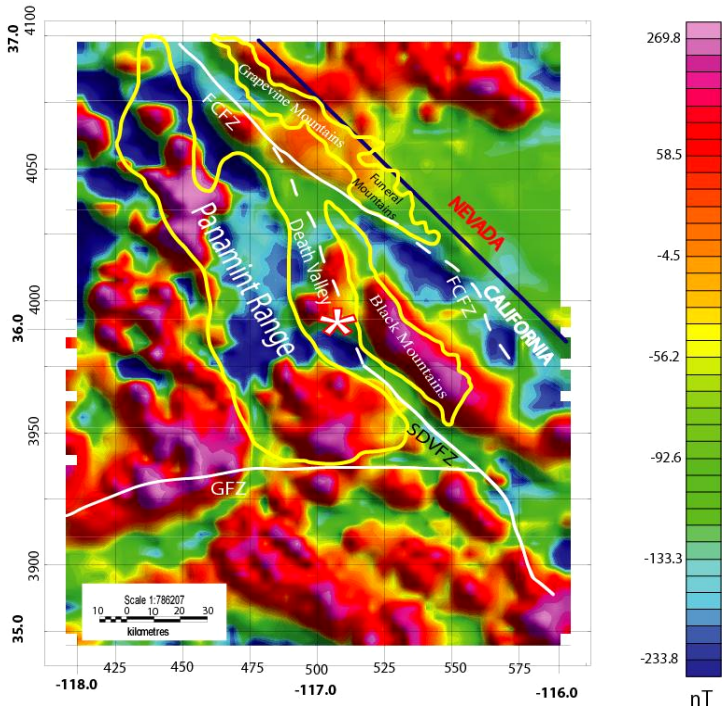


**Figure 6. Aeromagnetic anomaly map of Death Valley area. The * is a magnetic low which coincides with the location of the Death Valley bright spot. FCFZ, Furnace Creek fault zone; SDVFZ, Southern Death Valley Fault zone; GFZ, Garlock Fault Zone.**

 

## 4. Model Development

We based our initial models on the seismic reflection interpretations [2,8,12,18] and the receiver function data.

### 4.1. Bouguer Gravity Anomaly Map

The Bouguer gravity values decrease from –80 mGal in the Black Mountains to –180 mGal to the west and north (**Figure 4**) of the Black Mountains. Low gravity anomalies are likely caused by unconsolidated sediments in the basins, metasedimentary and granitic rocks, or by thicker crust or some combination of these features. Thus, the observation that the gravity values are significantly lower over the Panamint Range than over the Black Mountains is consistent with the interpretations [3,4,38] that the Panamint Range is comprised primarily of upper crustal rocks that have moved off the lower crustal rocks now exposed in the Black Mountains.

Other features of interest are the continuity of the large amplitude gravity and magnetic anomalies along the southern Death Valley fault zone and into the Mojave terrane and the well defined alignment of anomalies along the Garlock fault zone. The Panamint Range and the Northern Death Valley fault zone are not as well defined by the potential field data as are the anomalies associated with the Black Mountains, southern Death Valley and Garlock fault zones. One possible explanation for these observations is that the Panamint Range and Northern Death Valley fault zones are shallow features or, at least, they involve greater thickness of upper crustal, low density materials than the Black Mountains and southern Death Valley regions. On the other hand, the Black Mountains and faults to the south may represent more crustal scale features that could bring high density mantle materials closer to the surface locally.

The Death Valley bright spot (**Figures 4** and **6**) corresponds to a gravity low (–120 to –130 mGal), which is consistent with the interpretation by [8] of a deep magma body. One concern is that the gravity low in central Death Valley basin could be due to the basin sediment material rather than deeper structures. To further explore the source of this low gravity anomaly we modeled the first 5 km of the crust in central and southern Death Valley region using gravity and magnetic data with the seismic data interpretation of [12] for line L9 (**Figure 1**). The potential field model and comparison (**Figure 7**)

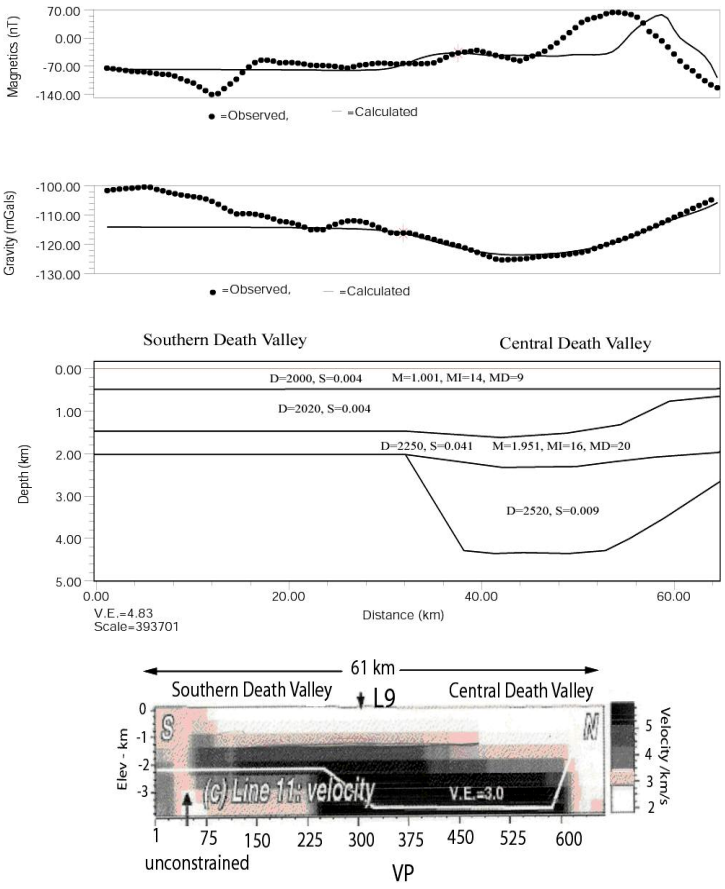


**Figure 7. Comparison model of the first 5 km of the crust from velocity model of Louie et al. (1997) Reference [12], for COCORP line 9-L9 (Figure 1), with density (D) and magnetic susceptibility (S) model in central and southern Death Valley.**

 

show a good match between the observed and calculated gravity data.

This suggests the gravity and magnetic anomalies are entirely due to the basin structure but it does not explain why the COCORP seismic data show an anomaly at 15 km depth and why a young volcanic cinder cone exists in the study area which is an indication of a magmatic material in the crust, additionally all the material beneath an observation site affects the gravity value. Thus, we chose to explore the model possibilities further.

## 4.2. Crustal Models

**Figure 4** shows the locations of two 2.5-dimensional (2.5-D) crustal models (**Figures 8** and **9**) across the bright spot constructed using a gravity and magnetic program developed by [39] and further revised by [40] and [41]. Gravity and magnetic values were extracted from the grid at 2-km intervals. These values were then input as observed data to the 2.5-D forward modeling program. The modeled profiles illustrate the general deep structure of the region and are not intended to reflect the detailed surface geology. Where seismic data are available, we have incorporated that information into the models. In general, gravity modeling produces non-unique results; however, we propose that by incorporating gravity, magnetic, receiver function, and seismic reflection/refracttion data, we can produce a well constrained model. Thus, as starting point in modeling, the depth to the Moho was determined from receiver functions, and the densities for the upper and lower crust and upper mantle were inferred from previous studies [12,19,42-44] and from the interpretation of the receiver function data, discussed previously. Magnetic susceptibilities were estimated from [43]. Our models are much longer than the area of interest in order to include the new knowledge of the Moho depths derived from the receiver functions.

We started modeling with initial densities from previous

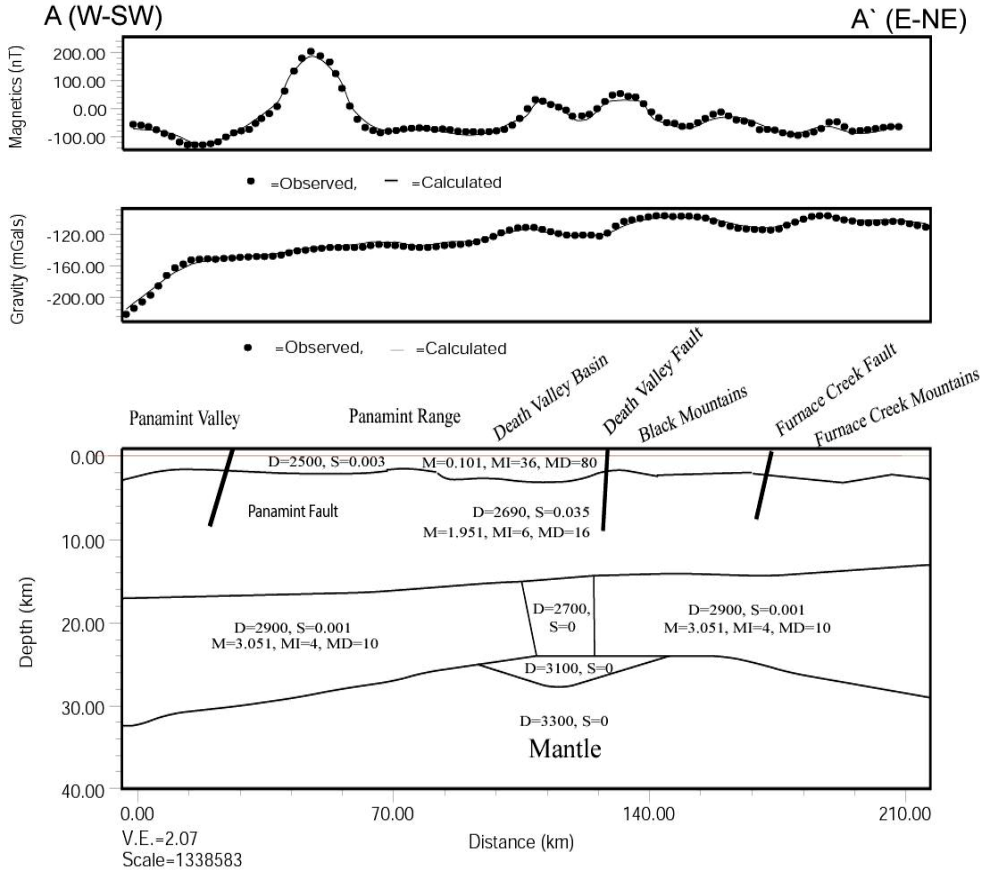


**Figure 8. Model A-A` (See Figures 4 and 5 for map view) is ~ 200 km long and covers the central part of the study area. The depth to the Moho is about 31 km at the starting point (A), decreases to 24 km in the central Death Valley basin and deepens to 33 km at the end point (A`). Low density material is found at the location of the bright spot and at a depth of 15 km; this low density material is underlain by a magma body (mafic underplating) at a depth of 24 to 25 km. (D = Density (kg/m3, S = Susceptibility (dimensionless), M = Magnetization (A/m), MI = Magnetic inclination (degrees), MD = Magnetic declination (degrees)).**

 

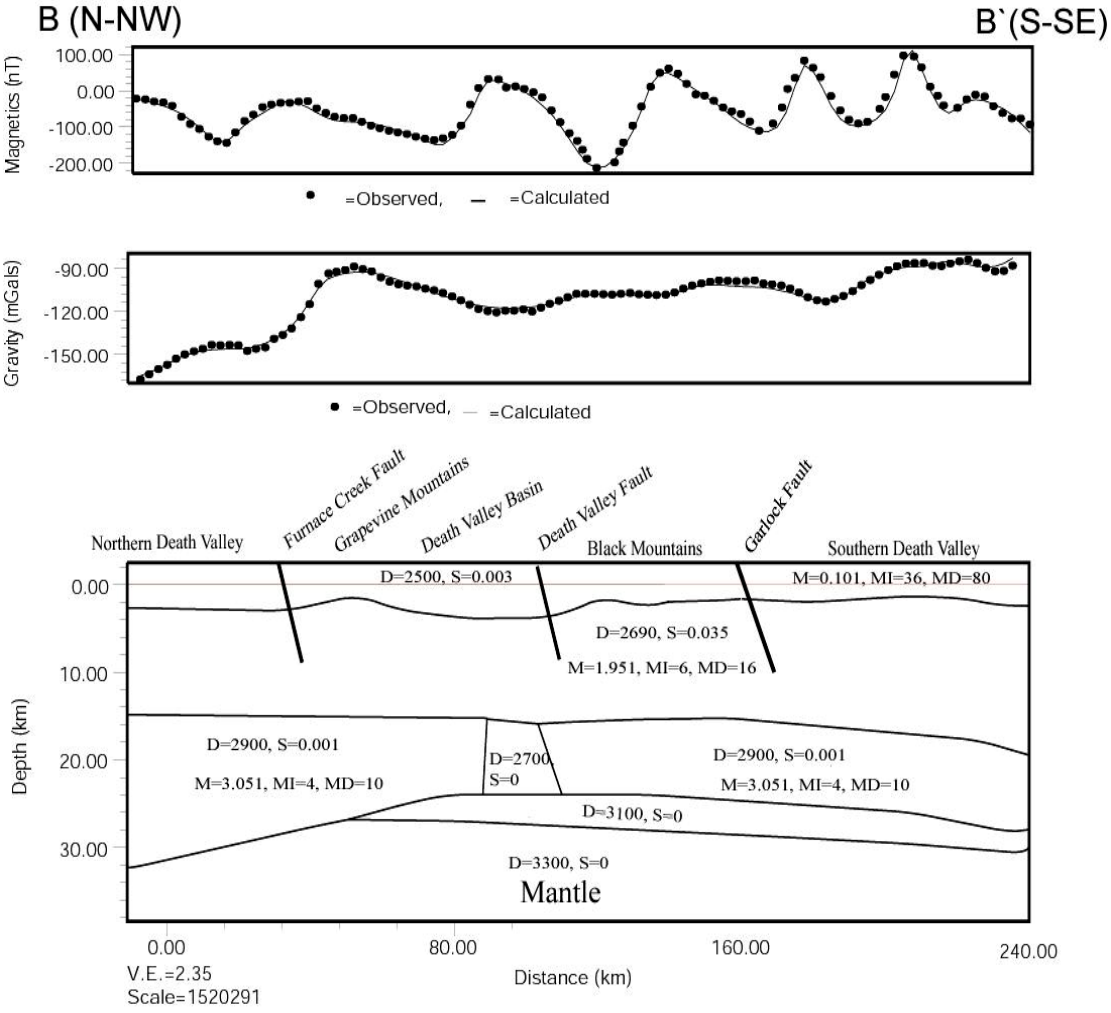


**Figure 9. Model B-B`(See Figures 4 and 5 for map view) is ~ 240 km long, perpendicular to model A-A`, and passes through the Death Valley and Black Mountains anomalies. The depth to the Moho is 34 km at the starting point (B), decreases to 24 km in the Death Valley basin and deepens to 28 km in the southern region of Death Valley at the end point (B`). Low density material is found at the location of the bright spot and at depth of 15 km; this low density material is underlain by a magma body (mafic underplating) at a depth of 24 to 25 km. (D = Density (kg/m3, S = Susceptibility (dimensionless), M = Magnetization (A/m), MI = Magnetic inclination (degrees), MD = Magnetic declination (degrees)).**

research and then changed these densities to minimize the difference between the observed and calculated data. Depth, density, and magnetic susceptibility were varied within 20% of initial values to determine a final model that best fit the receiver function, gravity and magnetic data. Density changes were required in the middleto-upper crust and upper mantle. The final models have a maximum misfit of approximately 2.0 mGal for the gravity, and about 6 nT for the magnetic data.

In our final interpretation, we had an average density of 2500 kg/m$^3$ for the basin sediments. We recognize that the density will vary and the thickness of the sedimentary basins also varies from over 1.5 km to 4 km. We used an estimated density in the location of the bright spot of 2360 kg/m$^3$ which represents the average density of the uppermost part of the upper crust. The density for the deeper part of the upper crust is estimated at 2690 kg/m$^3$. The lower crust density is estimated to be 2900 kg/m$^3$, the underplated materials density is estimated to be 3100 kg/m$^3$, while the estimated density of the inferred magma body at the bright spot location is 2700 kg/m$^3$. The density in the location of the inferred magma chamber that may be the source of the seismic bright spot could be affected by the temperature and amount of melt present. The modeled strike length for sedimentary basins ranges from 5 to 7 km and the strike length for the inferred bright spot magma

 

chamber is 5 km and is symmetrical about the profile.

### 4.3. Profile Interpretation

Model A-A` (**Figure 8**) is ~200 km long extending from near the eastern side of the Sierra Nevada Mountains in California to the Spring Mountains in Nevada. Within this region, the depth to the Moho is about 31 km in the west, decreases to 24 km in central Death Valley basin and deepens to 33 km at the eastern end of the model as suggested by the receiver function data. Model B-B` (**Figure 9**) is ~240 km long, perpendicular to model A-A`, and passes through Death Valley and the Black Mountains. The depth to the Moho is 34 km at the starting point near the Grapevine Mountains, decreases to 24 km in the Death Valley basin and deepens to 28 km in the Mojave Desert region at the end point (B`) of the model. These Moho depths are consistent with the receiver function data which suggests the Moho is shallow and, possibly, domed or flat-topped in shape in the central Death Valley basin. The flat-topped dome shape beneath the area of active upper crust extension is suggested to be primarily the product of magmatic activity in the lower crust and upper mantle [22].

Model B-B` (**Figure 9**) shows variations in the lower crustal depths in response to areas of uplifted basement in the Black Mountains and Funeral Mountain areas. Reference [19] hypothesized that the magnetic anomaly over the Black Mountains originates from rocks that were once part of a deep, relatively mafic crust that was subsequently brought closer to the surface by denudation and uplift. The southern region of Death Valley has large amplitude gravity and magnetic anomalies which reflect the most intense tectonic activity in the region. Variations in the potential field data are also modeled as due to active faulting. Fault locations in both models were determined from the geological data and from the offset of the upper and lower crust. In addition, faults that offset lithologies with moderate or high magnetic susceptibilities often produce small magnetic anomalies useful for identification and mapping of faults [43].

We modeled low density, non-magnetic material, inferred to be partially molten, at the location of the bright spot below a depth of approximately 15 km. This interpretation is supported by a combined gravity and magnetic low in that location. Curie point depth estimation in Death Valley [45] indicates the Curie point is 12 - 15 km in the central area of Death Valley, which is also consistent with high temperatures and possible partial melting at shallow depths. We expect the gravity low is caused by both the shallow basin sediment and deep structures. To create an acceptable model of the inferred magmatic body we tested several scenarios in constructing our models; in one scenario we remove the magmatic body from the model and in another scenario we change the thickness of the magmatic body. In both scenarios we could not match the observed and calculated data. However, in our models this inferred magmatic material is compensated by additional of magma at a depth of 24 to 25 km and this also provides an acceptable fit to the available data. This deeper magma body is inferred to be a mixture of lower crust and upper mantle material. To fit this body to our models we presumed the density of this body to be 3100 kg/m$^3$. The deeper magmatic body suggests mafic underplating of the crust and extends for about 60 km in SW-NE direction (**Figure 8**), and at least 160 km in NW-SE direction (**Figure 9**). This magma body is likely to be the mantle source of the magma that gives rise to the bright spot of Death Valley.

## 5. Conclusions

We combined receiver function, gravity, magnetic data, and pre-existing seismic interpretations to study an area of Death Valley where previous studies [2,8] have suggested there may be a magma body but later studies in the region have not supported that interpretation. Our study suggests the presence of magma in the lower crust is reasonable if it is combined with underplating of the lower crust. The primary evidence is that the receiver functions indicate the Moho is shallow near the inferred magma chamber and gravity and magnetic lows in that region are consistent with the interpretation of magma. The Moho appears to form a dome centered beneath the southern and central Death Valley basins. The focus of crustal thinning beneath the area of active upper crust extension is suggested to be primarily the product of magmatic activity in the lower crust which weakens the crust and causes it to stretch. The region of possible magmatic underplating associated with the inferred magma body extends for about 60 km in SW-NE direction, and more than 160 km in NW-SE direction. Our models are not unique and were created based on the available data. The central basin of Death Valley is poorly covered with re- ceiver function stations and, thus, we estimated a 24 km depth based on contouring the available data from stations surrounding the study area. To confirm the existence of the molten or partial melt material within the lower crust additional geophysical data are needed.

## 6. Acknowledgements

We would like to thank Dr. Terry Pavlis, Dr. William Cornell and Dr. Vladik Kreinovich for helpful discussion. We would like also to thank Dr. Raed Al-Douri and Carlos Montana for the technical support. The work was

 

partially supported by NSF grant number HRD-0734825.

## 7. References

[1] L. Serpa and B. deVoogd, "Deep Seismic Reflection Evidence for the Role of Extension in the Evolution of Continental Crust," *Royal Association Society Geophysical Journal*, Vol. 89, No. 1, 1987, pp. 55-60.

[2] L. Serpa, B. de Voogd, L. Wright, J. Willemin, J. Oliver, E. Hauser and B. Troxel, "Structure of the Central Death Valley Pull apart Basin and Vicinity from the COCORP Models in the Southern Great Basin," *Geological Society of America Bulletin*, Vol. 100, No. 9, 1988, pp. 1437-1450. doi:10.1130/0016-7606(1988)100<1437:SOTCDV>2.3.CO;2

[3] J. Snow and B. Wernicke, "Uniqueness of Geologic Cor-Relation: An Example from the Death Valley Extended Terrain," *Geological Society of America Bulletin*, Vol. 101, No. 11, 1989, pp. 876-885.

[4] L. Serpa and T. Pavlis, "Three-Dimensional Model of the Late Cenozoic History of the Death Valley Region, South-Eastern California," *Tectonics*, Vol. 15, 1996, pp. 1113-1128. doi:10.1029/96TC01633

[5] L. Wright, R. Greene, I. Cemen, F. Johnson, A. Prave and R. Drake, "Tectonostratigraphic Development of the Miocene-Pliocene Furnace Creek Basin and Related Features, Death Valley Region, California," In: L. Wright and B. Troxel, Eds., *Cenozoic Basins of the Death Valley Region*, Geological Society of America Special Paper 333, 1996, pp. 115-126.

[6] G. Miller, "Basement-Involved Thrust Faulting in a Thin-Skinned Fold-and-Thrust Belt, Death Valley, California, USA," *Geology*, Vol. 31, No. 1, 2003, pp. 31-34. doi:10.1130/0091-7613(2003)031<0031:BITFIA>2.0.CO;2

[7] M. Miller and T. Pavlis, "The Black Mountains Turtlebacks: Rosetta Stones of Death Valley Tectonics," *Earth Science Reviews*, Vol. 73, No. 1-4, 2005, pp. 115-138. doi:10.1016/j.earscirev.2005.04.007

[8] B. de Voogd, L. Serpa, L. Brown, E. Hauser, S. Kaufman, J. Oliver, B. Troxel, B. Willemin and L. Wright, "The Death Valley Bright Spot; A Midcrustal Magma Body in the Southern Great Basin, California," *Geology*, Vol. 14, No. 1, 1986, pp. 64-67. doi:10.1130/0091-7613(1986)14<64:DVBSAM>2.0.CO;2

[9] T. Brocher, P. Hart and S. Carle, "Feasibility Study of the Seismic Reflection Method in Armargosa Desert, Nye County, Nevada," U.S. Geological Survey Open-File Report, 1990, pp. 89-133.

[10] S. Park, "Mantle Heterogeneity beneath Eastern California from Magnetotelluric Measurements," *Journal of Geophysical Research*, Vol. 109, No. B09406, 2004, pp. 1-13. doi:10.1029/2003JB002948

[11] S. Park and B. Wernicke, "Electrical Conductivity Image of Quaternary Faults and Tertiary Detachments in the California Basin and Range," *Tectonics*, Vol. 22, No. 4, 2003, pp.1-17. doi:10.1029/2001TC001324

[12] J. Louie, S. Pullammanappallil and W. Honjas, "Velocity Models for the Highly Extended Crust of the Death Valley, California," *Geophysical Research Letters*, Vol. 24, No. 7, 1997, pp. 735-738. doi:10.1029/97GL00574

[13] B. Burchfiel and J. Stewart, "Pull-Apart Origin of the Central Segment of the Death Valley, California," *Geological Society of America Bulletin*, Vol. 77, No. 4, 1966, pp. 439-442. doi:10.1130/0016-7606(1966)77[439:POOTCS]2.0.CO;2

[14] C. Keener, L. Serpa and T. Pavils, "Faulting at Mormon point, Death Valley, California: A Low-Angle Normal Fault Cut by a High-Angle Fault," *Geology*, Vol. 21, No. 4, 1993, pp. 327-330. doi:10.1130/0091-7613(1993)021<0327:FAMPDV>2.3.CO;2

[15] L. Wright and B. Troxel, "Shallow-Fault Interpretation of Basin and Range Structure Southwestern Great Basin," In: K. A. Dejon and R. Scholten, Eds., *Gravity and Tectonics*, John Wiley and Sons, New York, 1973, pp. 397-407.

[16] Z. Sylvester, "Facies, Architecture and Bed-Thickness Structure of Turbidity Systems: Examples from the East Carpathian Flysch, Romania, and the Great Valley Group, California," Ph.D. Dissertation, Stanford University, Stanford, 2001.

[17] C. Hunt and D. Mabey, "Stratigraphy and Structure, Death Valley California," US Geological Survey Professional Paper 494-A, U.S. Government Printing Office Washington, DC, 1966.

[18] E. Geist and T. Brocher, "Geometry and Subsurface Lithology of Southern Death Valley Basin, California, Based on Refraction Analysis of Multichannel Seismic Data," *Geology*, Vol. 15, No. 12, 1987, pp. 1159-1162. doi:10.1130/0091-7613(1987)15<1159:GASLOS>2.0.CO;2

[19] R. Blakely, R. Jachens, J. Calzia and V. Langenheim, "Cenozoic Basins of the Death Valley Extended Terrane as Reflected in Regional-Scale Gravity Anomalies," In: L.A. Wright and B. W. Troxel, Eds., *Cenozoic Basins of the Death Valley Region*, Geological Society of America Special Paper, Boulder, Vol. 333, 1999, pp. 1-16.

[20] L. Serpa, "The Three Dimensional Geometry of the Garlock Fault Zone," *Geological Society of America Abstract with Programs*, Vol. 19, 1987, p. 838.

[21] B. deVoogd, L. Serpa and L. Brown, "Crustal Extension and Magmatic Processes: COCORP Profiles from Death Valley and the Rio Grande Rift," *Geological Society of American Bulletin*, Vol. 100, No. 10, 1988, pp. 1550-1567. doi:10.1130/0016-7606(1988)100<1550:CEAMPC>2.3.CO;2

[22] L. Serpa, "Structural Styles Across an Extensional Orogen; Results from the COCORP Mojave and Death Valley Seismic Transects," In: B. P, Wernicke, Ed., *Basin and Range Extensional Tectonics near the Latitude of Las Vegas, Nevada*, Geological Society of America Memoir

 

176, Boulder, 1990, pp. 335-344.

[23] F. O'Doherty and A. Anstey, "Reflections on Amplitudes," *Geophysical Prospecting*, Vol. 19, No. 3, 1971, pp. 430-458. doi:10.1111/j.1365-2478.1971.tb00610.x

[24] W. Ewing, W. Jardetsky and F. Press "Elastic Waves in Layered Media," McGraw-Hill, New York, 1957, p. 380.

[25] B. Crowe, S. Self, D. Vaniman, R. Amos and F. Perry, "Aspects of Potential Magmatic Disruption of a High Level Radioactive Waste Repository in Southern Nevada," *Journal of Geology*, Vol. 91, No. 3, 1983, pp. 259-276. doi:10.1086/628770

[26] C. Herzberg, W. Fyfe and M. Carr, "Density Constraints on the Formation of the Continental Moho and Crust," *Contributions to Mineralogy and Petrology*, Vol. 84, No. 1, 1983, pp. 1-5. doi:10.1007/BF01132324

[27] C. Ammon, G. Randall and G. Zandt, "On the Nonuniqueness of Receiver Function Inversions," *Journal of Geophysical Research*, Vol. 95, No. B10, 1990, pp. 15303-15318. doi:10.1029/JB095iB10p15303

[28] L. Zhu and H. Kanamori, "Moho Depth Variation in Southern California from Teleseimic Receiver Functions," *Journal of Geophysical Research*, Vol. 105, No. B2, 2000, pp. 2969-2980. doi:10.1029/1999JB900322

[29] J. Ligorria and C. Ammon, "Iterative Deconvolution and Receiver Function Estimation," *Bulletin of Seismological Society of America*, Vol. 89, No. 5, 1999, pp. 1395-1400.

[30] L. Zhu, "Estimation of Crustal Thickness and Vp/Vs Ratio beneath the Tibetan Plateau from Teleseismic Converted Waves," *EOS Transactions of AGU*, Vol. 74 No. 16, 1993.

[31] G. Zandt, S. Myers and T. Wallace, "Crust and Mantle Structure across the Basin and Range Colorado Plateau boundary at 37º N Latitude and Implication for Cenozoic Extensional Mechanism," *Journal of Geophysical Research.*, Vol. 100, No. B6, 1995, pp. 10529-10548. doi:10.1029/94JB03063

[32] G. Zandt and C. Ammon, "Continental Crust Composition Constrained by Measurements of Crustal Poisson Ratio," *Nature*, Vol. 374, 1995, pp. 152-154. doi:10.1038/374152a0

[33] D. Eaton, S. Dineva and R. Mereu, "Crustal Thickness and Vp/Vs Variations in the Grenville Orogen (Ontario, Canada) from Analysis of Teleseismic Receiver Functions," *Tectonophysics*, Vol. 420, No. 1-2, 2006, pp. 223-238. doi:10.1016/j.tecto.2006.01.023

[34] T. Nakajima, A. Matsuzawa, A. Hasegawa and D. Zaho, "Three Dimensional Structure of Vp, Vs and Vp/Vs beneath Northeastern Japan: Implications for Arc Magmatism and Fluids," *Journal of Geophysical Research*, Vol. 106, No. B10, 2001. pp. 21843-21857. doi:10.1029/2000JB000008

[35] W. Webring, "MINC, a Gridding Program Based on Minimum Curvature," U.S. Geological Survey Open-File Report, U.S. Geological Survey, Denver, 1982, pp. 81-1224,

[36] D. Plouff, "Preliminary Documentation for a FORTRAN Program to Compute Gravity Terrain Corrections Based on Topography Digitized on a Geographic Grid," U.S. Geological Survey Open File Report, U.S. Geological Survey, Denver, 1977, pp. 77-535.

[37] V. Bankey, A. Cuevas, D. Daniels, C. Finn, I. Hernandez, P. Hill, R. Kucks, W. Miles, M. Pilkington, C. Roberts, W. Roest, V. Rystrom, S. Shearer, S. Snyder, R. Sweeney, J. Velez, J. Phillips and D. Ravat, D, "Digital Data Grids for the magnetic Anomaly187 Map of North America," U.S. Geological Survey Open-File Report 02-414, U.S. Geological Survey, Denver, 2002.

[38] D. Holm and B. Wernicke, "Black Mountains Crustal section, Death Valley Extended Terrain, California," *Geology*, Vol. 18, No. 6, 1990, pp. 520-523. doi:10.1130/0091-7613(1990)018<0520:BMCSDV>2.3.CO;2

[39] M. Talwani, J. Worzel and M. Landisman, "Rapid Gravity Computations for Two Dimensional Bodies with Appli Cations to the Mendocino Submarine Fracture Zone," *Journal of Geophysical Research*, Vol. 64, No. 1, 1959, pp. 49-59. doi:10.1029/JZ064i001p00049

[40] L. Pedersen, "Interpretation of Potential Field Data, a Generalized Inverse Approach," *Geophysical Prospecting*, Vol. 25, No. 2, 1977, pp. 199-230. doi:10.1111/j.1365-2478.1977.tb01164.x

[41] J. Cady, "Calculation of Gravity and Magnetic Anomalies of Finite-Length Right Polygonal Prisms," *Geophysics*, Vol. 45, 1980, pp. 1507-1512. doi:10.1190/1.1441045

[42] K. Mickus and W. James, "Regional Gravity Studies in Southern California, Western Arizona and Southern Nevada," *Journal of Geophysical Research*, Vol. 96, No. 12, 1991, pp. 333-350.

[43] R. Blakely, V. Langenheim, D. Ponce and G. Dixon, "Aeromagnetic Survey of the Amargosa Desert, Nevada and California: A Tool for Understanding near Surface Geology and Hydrology," U. S. Geological Survey Open-File Report 00-188, U.S. Geological Survey, Denver, 2000.

[44] D. Ponce and R. Blakely, "Aeromagnetic Map of Death Valley Ground Model Area. Nevada and California," U. S. Geological Survey, Miscellaneous Field Studies MF-2381-D, 2001.

[45] M. Hussein, "Integrated and Comparative Geophysical Studies of Crustal Structure of Pull-Apart Basins: The Salton trough and Death Valley, California Regions," Ph.D. Dissertation, University of Texas at El Paso, El Paso, 2007.

 

**Websites:**
NSF "Earthscope," 2003, 18 June 2006 <http//www.earthscope.org/>
NSF, "Earthscope Automated Receivers Survey (EARS)," 2003. 18 June 2006 http://www.ears.iris.washington.edu
UTEP "Pan-American Center for Earth and Environmental studies" 19-Jul-2005. Aug-20-2006. http://www.research.utep.edu/paces

 